

Effect of 3,5-dinitrosalicylic Acid on Silver Plating in Methanesulfonic Acid

Jialun Wu¹, Daoxin Wu^{1*}, Ronghua Yang¹, Yinjie Kuang¹, Zhongliang Xiao¹, Yong Huang², Jiayu Zhu¹, Xin Li¹

¹ School of Chemistry and Food Engineering, Changsha University of Science and Technology, Changsha, 410114, P. R. China

² Hunan Provincial Engineering Technology Research Center for Printed Circuit Board (PCB), Aoshikang Technology Company, Yiyang, 413000, P. R. China

*E-mail: daoxinwu@126.com

Received: 2 February 2020 / Accepted: 22 March 2020 / Published: 10 June 2020

The systematic electrochemical methods were used to explain the complicated heterogeneous nucleation mechanism caused by displacement plating. Here, the effect of 3,5-dinitrosalicylic acid (DNS) on displacement silver plating on copper substrate in methanesulfonic acid is studied. Results show that DNS affects anode process by absorbing the copper surface to hinder silver deposition. The diffusion coefficient of silver ions and nucleus density of silver significantly decrease with the increase of DNS concentration. The crystalline EN with a large potential shift indicates the loose and uneven structure of silver deposition. By contrast, the EN with a small potential shift indicates the dense layer. The energy distribution plot based on wavelet transform shows that the accumulated relative energy in region C decreases and that in region A significantly increases with the increase of DNS concentration. This finding indicates that DNS facilitates the transition of system control from diffusion control to activation control. The nucleation mechanism of silver deposition changes from partial instantaneous nucleation and partial progressive nucleation to complete progressive nucleation with the 3D nucleation mode. Understanding the mechanism of displacement silver plating on copper is therefore important.

Keywords: Silver plating; Electrochemical impedance spectroscopy; Nucleation mechanism; Electrochemical noise

1. INTRODUCTION

Printed circuit boards (PCBs) are widely used in electronic products. However, the physical and chemical properties of PCBs usually deteriorate due to the easy oxidation of copper surfaces. As an important surface treatment technology of PCBs, silver plating can improve the oxidation resistance, electrical conductivity, and thermal stability of PCB metal surfaces [1–7]. Silver plating can be

categorized as displacement plating [5–9], vapor deposition [10], electroplating [11–15], and reduction plating [16–18]. Among these methods, displacement plating has attracted wide attention because of its advantages, such as low equipment requirement, simple operation, and low energy consumption. However, the rate of displacement reaction is excessively fast due to the large potential difference between copper and silver, resulting in a loose and non-uniform coating structure of silver deposition. The addition of appropriate additives to the metal-plating such as silver-plating solution is important to obtain a dense and uniform coating [19–21]. For example, Hai et al. obtained a dense and uniform silver coating by adjusting the molar ratio of $\text{NH}_4\text{OH}/(\text{NH}_4)_2\text{SO}_4$, activation time, and feed rate of the silver ion solution [6]. Zhao used PVP and citric acid as additives to control the deposition rate of silver [7]. John achieved fine deposits of silver by using linear aliphatic amines as additives [22].

The mechanism of heterogeneous nucleation reaction produced from displacement silver plating is complicated due to the particularity of displacement reaction in the electroless plating process, complexity of reaction system, and difficulty to accurately control the reaction process. Xu et al. proposed that the reduction reaction of silver was dominated by the dissolution of copper surface oxides and hydroxides and the coating method itself in an ammonia solution [23]. Although the results presented by these methods can explain the structure and crystal orientation of the coating, no essential description of the heterogeneous nucleation of replacement silver plating is available, and explaining the issue through the angle of dynamics is insufficient. At present, few studies discuss the mechanism of displacement silver plating on copper substrate. Electrochemical methods, such as electrochemical impedance spectroscopy (EIS), potentiodynamic curve, chronoamperometry, chronocoulometry, and voltammetry, are often used to investigate the mechanism of silver electrodeposition [11,12,24–32]. However, the above methods do not attract sufficient attention in the study of displacement plating mechanism. At present, the understanding on how additives affect the nucleation and growth mechanism of silver crystals during displacement silver plating is still lacking. Therefore, the nucleation, growth, and activation control mechanism of displacement silver plating crystallization process through the electrochemical methods presented above combined with the electrochemical noise technology based on wavelet analysis should be studied [33].

In this work, 3,5-dinitrosalicylic acid (DNS) was selected as an additive during displacement silver plating on copper substrates. The role of DNS in the reaction was investigated through cyclic voltammetry, EIS, and potentiodynamic polarization. Moreover, the nucleation mechanism of silver was studied through chronoamperometry. The surface information of coating structure and distribution of crystal cell energy were further obtained by electrochemical noise based on wavelet transform to understand the effect of DNS on the nucleation and crystal growth of silver during crystallization.

2. EXPERIMENTAL

2.1 Materials

All materials including purple copper sheets, ethanol, silver oxide, methanesulfonic acid, 3,5-dinitrosalicylic acid (DNS), potassium hydroxide and epoxy resin were purchased from Aldrich (USA).

2.2 Silver plating on copper substrate

The purple copper sheet with 99.99% purity was polished to remove oxide film on the surface. After cleaning with deionized water and ethanol, the copper sheet was dried with cold air and sealed in a dry environment for 24 hours to obtain a bright and neat surface. Before use, the copper sheet was cut into small pieces with a size of 1cm×4 cm and sealed by epoxy resin in the middle part with a size of 1cm×2 cm. A plating solution containing 0.01M silver ions (silver ions were derived from silver oxide dissolved in 0.5M methanesulfonic acid solution) was adjusted by KOH to pH 0.3. DNS was used as an additive for displacement silver plating, and its concentration was 0.5, 2 and 6mM. All solutions were prepared with deionized water.

2.3 Electrochemical measurements of the silver plating

Displacement silver plating on the copper surface was characterized through electrochemical methods of cyclic voltammetry (the scanning rate 0.1 V/s, the voltage range -0.8 V~0.2 V), EIS (the frequency 0.01 - 100000 Hz under open circuit potential), chronoamperometry (cathodic overpotential), potentiodynamic polarization (open circuit potential), and electrochemical noise (the sampling frequency 4Hz). All electrochemical measurements were implemented in a three-electrode system in which a copper sheet was used as the working electrode, a platinum sheet was used as the counter electrode, and Ag/AgCl was used as the reference electrode. The experiments were performed in the static solution at 25°C on the electrochemical workstation (CHI660D, Shanghai Chenhua Instrument Co., Ltd.) for three times. The surface morphology of copper was observed by a scanning electron microscope (SEM, Hitachi SU70).

3. RESULTS AND DISCUSSION

With the addition of DNS in the plating solution, the silver coating on the copper surface significantly changed, as shown in Fig. 1. Fig. 1A shows a photograph of the silver plating on copper sheets without DNS addition. Numerous black spots and almost no silver white spots are seen on the surface of the copper, indicating that the silver layer structure is poorly dense. With the increase of DNS concentration, the black spots on the copper surface decreased and silver-white spots gradually appeared, finally forming a bright silver color at 6mM DNS concentration, as shown in Fig. 1B–1D. This evident difference indicates that DNS has a good promoting effect on the displacement silver plating of copper sheet surface and high DNS concentrations are favorable for depositing silver on the copper sheet.

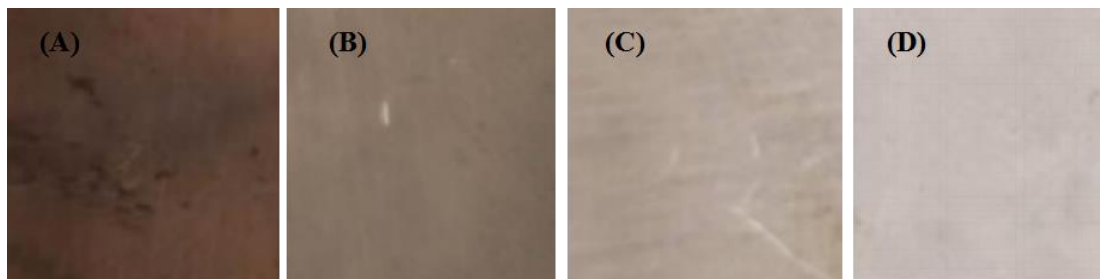


Figure 1. Microscopic photographs of silver-plating on copper sheet which were processed beforehand that included microetching and degreasing at different DNS concentrations in methanesulfonic acid: A-0mM; B-0.5mM; C-2mM; D-6mM; magnification: $\times 10$.

3.1 Cyclic voltammogram

The effect of DNS on the electroless silver plating on copper was preliminarily investigated through cyclic voltammetry and the results were shown in Fig. 2. The black arrow in the plot indicates the direction of potential scanning. From curve 1 without addition of DNS, the peak current of anodic oxidation evidently increases when the positive sweep potential exceeds -0.05 V. At the same time, two distinct reduction current peaks are observed when the negative sweep occurs. The peak from -0.175 V to -0.275 V during the negative sweep process is attributed to reduction of silver ions in the solution. With increasing the DNS concentration in the plating solution, the current density of anodic oxidation in cyclic voltammetry curve significantly decreases. At the same time, the current density of silver ion reduction also decreases, and the potential negatively shifts. Hence, DNS can significantly inhibit the anodic dissolution process of copper and the cathodic reduction reaction of silver ions because the contact area of silver ions on the copper surface is decreased due to the adsorption of DNS on the copper surfaces [34].

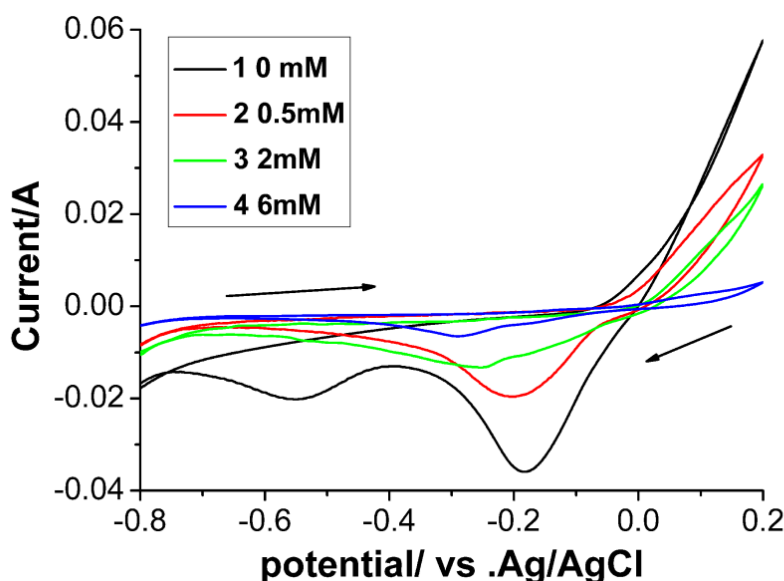


Figure 2. Cyclic voltammogram curves of silver deposition on copper at a scan rate of 0.1 V/s for a series of DNS concentrations.

3.2 Potentiodynamic polarization measurements

To further understand the influence of DNS on the displacement silver plating process, potentiodynamic polarization was adopted and the results were shown in Fig. 3. The open circuit potential evidently shifts to the positive direction with increasing the concentration of DNS in solution. Moreover, the slope of the anode potentiodynamic curve is much larger than that of the cathode potentiodynamic curve. Hence, the inhibition of DNS on the anodic reaction is much greater than that on the cathodic reaction. The results from fitting the potentiodynamic polarization curves, as shown in Table 1, further confirm this result. When the DNS concentration increases from 0 mM to 6 mM, the rate of anodic reaction decreases by 28.4% (from 0.546 to 0.391 mA), which is much larger than that of the cathode reaction by 10.42% (from 4.261 to 3.817 mA). The potentiodynamic polarization results show that DNS simultaneously inhibited the cathodic reduction reaction and anodic dissolution of copper during displacement silver plating, but the inhibition on the latter is predominant.

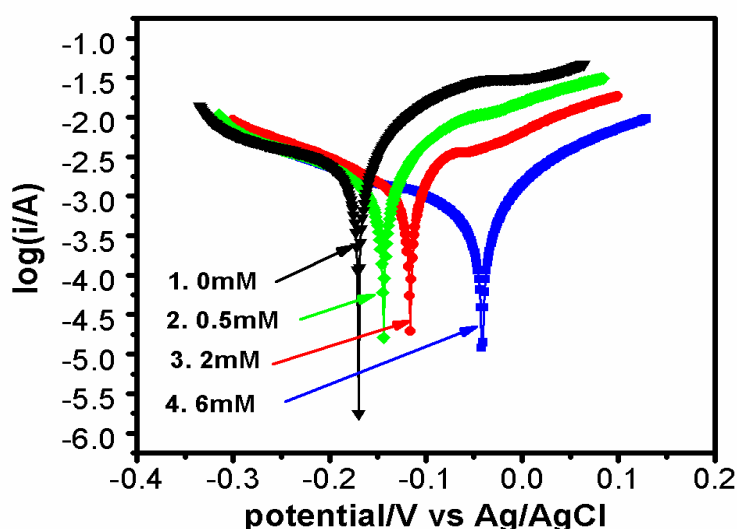


Figure 3. Polarization curves for silver-plating at different DNS concentrations in methanesulfonic acid.

Table 1. Some parameters obtained from the potentiodynamic curves

C(mM)	i_c^0 (mA)	i_a^0 (mA)	Open circuit potential (V)
0	4.261	0.546	-0.169
0.5	3.981	0.513	-0.144
2	3.949	0.423	-0.116
6	3.817	0.391	-0.042

3.3 EIS

EIS was used to further explain the role of DNS in displacement silver plating, and the results were shown in Fig. 4. The EIS consists of two capacitive reactance arcs when there is no additive. The arc in the high-frequency region corresponds to the reduction reaction of silver ions. Meanwhile, the arc

in the middle- and low-frequency regions corresponds to the oxidation reaction of copper. An evident inductive reactance arc is observed in the low-frequency region of the EIS diagram with the addition of DNS, indicating the adsorption of DNS on the surfaces of the copper. The diameter of capacitive reactance arc in the middle-frequency region significantly increases with the increase of DNS concentration. Hence, the anodic oxidation process of copper is evidently inhibited. The possible reason is that DNS was adsorbed on the surface of copper, thereby hindering the transfer of electrons from the copper matrix to the copper/plating solution interface and subsequently inhibiting its dissolution [35]. However, the large arc in the middle-frequency region also contains a small one, which is generated by bivalent copper ions from the oxidation of monovalent copper ions. At the same time, the diameter of the arc in the high-frequency region increases, but the increase of amplitude is much smaller than that in the medium-frequency region. Therefore, the inhibition effect of DNS on the anode process is greater than that on the cathode process. The result is agreement with the results obtained from the potentiodynamic polarization analysis.

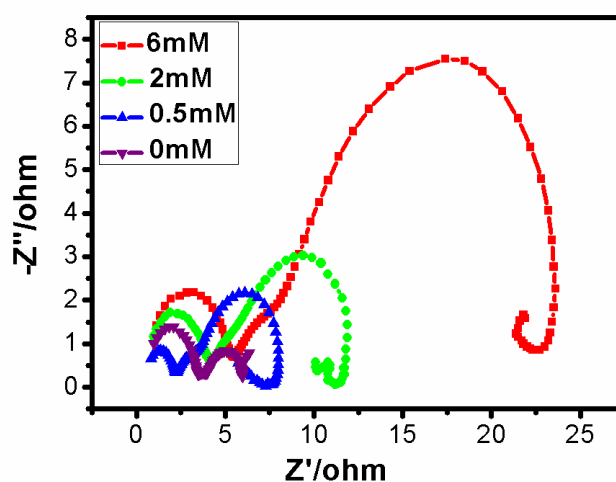


Figure 4. AC impedance spectrum for silver-plating on copper at different DNS concentrations in methanesulfonic acid. Test parameters: central potential: open potential, frequency range: 0.01-100000Hz, amplitude: 5mV.

3.4 Electrochemical noise

The quantity of additives generally affects the deposition process of silver. Additives can change the silver-plated layer structure from the loose dendritic structure to the dense and delicate structure. The electrochemical noise technique is an effective method for in situ crystallization research. Fig.5 shows the EN features in time domain. The crystalline EN with the large potential shift indicates the loose and uneven structure of the silver deposit, whereas the EN with the small potential shift indicates the dense layer. As the DNS concentration increases, the sediment structure changes from dendritic particles to a dense layer structure, as shown in the SEM images of Fig. 6.

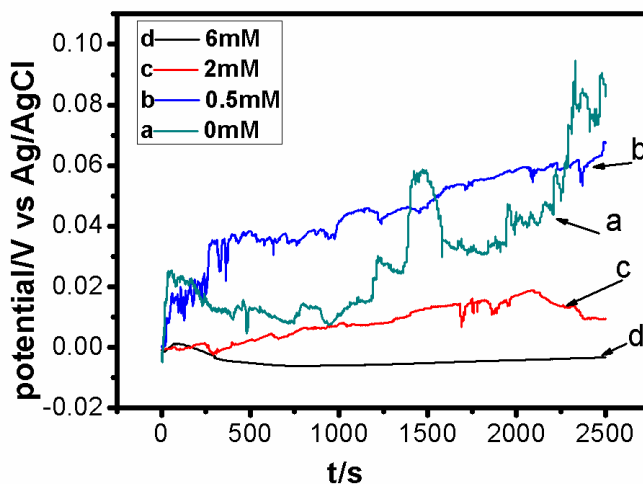


Figure 5. Electrochemical potential noise of silver deposition on a copper substrate in a series of DNS concentrations.

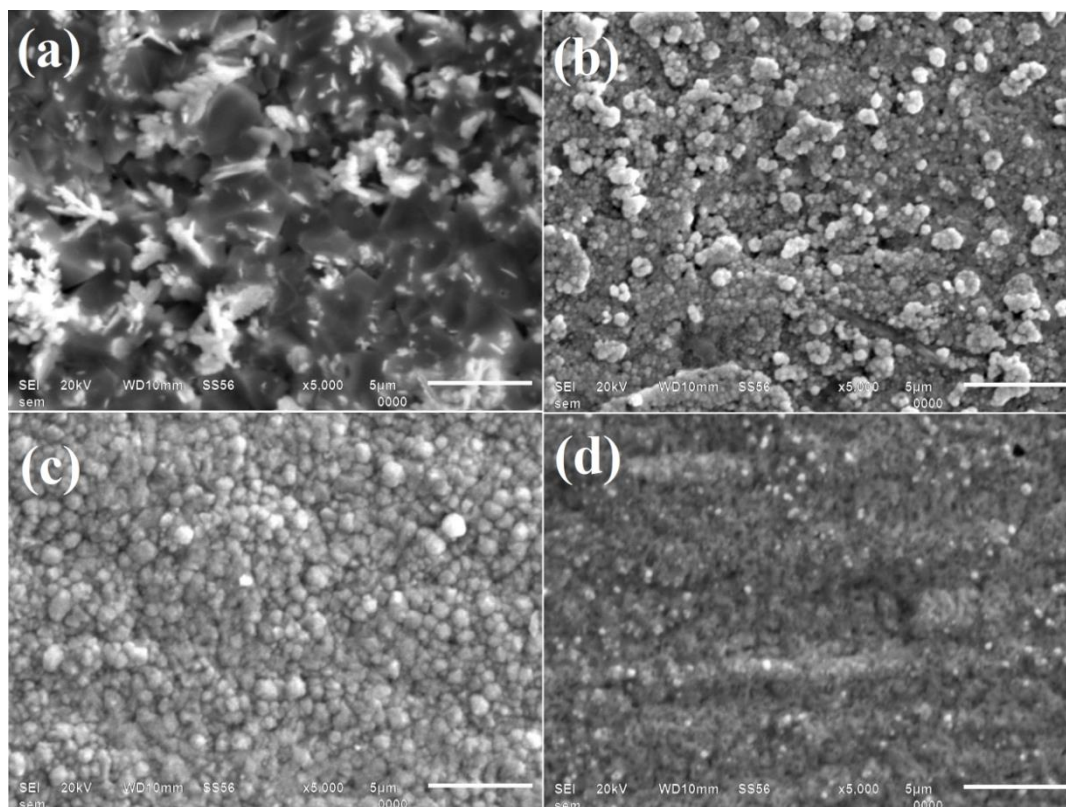


Figure 6. SEM micrographs of Ag layers deposited on copper at 20kV from methanesulfonic acid bath with different DNS concentrations: (a) 0mM; (b) 0.5mM; (c) 2mM; (d) 6mM.

For the purpose of characterizing the electrocrystalline EN in detail and effectively eliminating effect of the current contribution derived from capacitance charging, the orthogonal db4 wavelet was chosen to calculate the wavelet transform and the overall energy noise[34,36–38].The plots of the relative energy accumulated by each crystal and the crystal name are called energy distribution plots

(EDPs). To remove the energy portion contributed by DC drift from the ensemble energy of the noise, the EDP was re-plotted by deducting the contribution portion caused by S_8 crystal from the ensemble signal energy. The noise data shown in Fig. 7 is the corresponding re-plotted EDP (RP-EDP). The RP-EDP can be classified into three sections in accordance with the difference of time constant from the silver deposition process: ① region A represents the nucleation process between D_1 and D_3 ; ② region B represents the growth process between D_3 and D_6 ; and ③ region C represents the diffusion process between D_6 and D_8 .

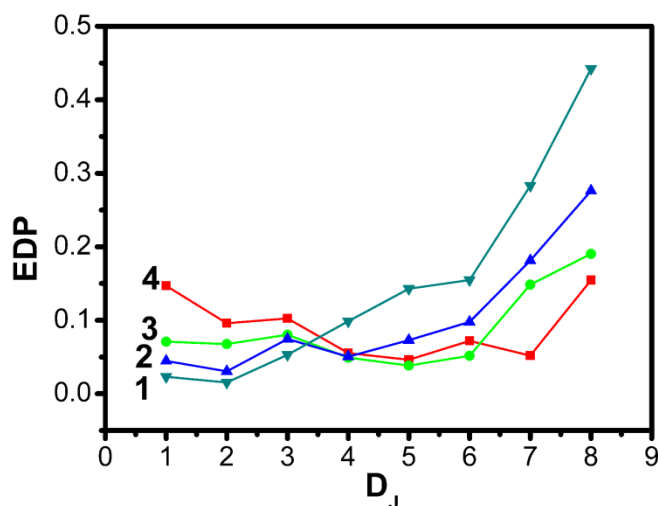


Figure 7. RP-EDP of silver deposition on a copper substrate in a series of DNS concentrations: 1-0mM; 2-0.5mM; 3-2mM; 4-6mM.

As shown in Fig. 6, the silver deposits consist of large aggregated particles with a dendritic or spongy structure when DNS is not present in the silver-plating system. The silver crystallization process is under the control of the diffusion process of Ag^+ to surface of copper from the bulk solution. The silver ions that reach the copper surface will preferentially discharge on the homogeneous crystallites or inhomogeneous sites which have relatively high Gibbs free energy, including the emergence points of edge, screw dislocation, and kink sites [34, 39]. As a result, the accumulation of relative energy and the formation of aggregate structure of silver deposits in regional C are higher than that in regional A.

When DNS is added to the silver-plating solution, it is preferentially adsorbed at the protrusion sites on the surfaces of copper, increasing the quantity of new nuclei and leads to local diffusion around the microcrystals. Therefore, the crystallization reaction of silver changes from diffusion control by mixing control to activation control with increasing the DNS concentration. The SEM images show that the grains are merged in the growth process of silver crystallization. Then, a dense silver-plating layer is formed. The amplitude EN and potential drift of crystallization decrease, and the structure of silver deposits changes from a dendritic to a dense cluster structure. Under this circumstance, the accumulated relative energy in domain C decreases, and the energy in region A significantly increases. Hence, the DNS facilitates the transition of system control step from diffusion control to activation control.

3.5 Nucleation mechanism

The nucleation and crystal growth process of silver can be clearly reflected by the corresponding potentiostatic transients. Faradaic current–time curves of silver deposited on copper in methanesulfonic acid with different DNS concentrations at a cathodic potential of -0.3V are represented in Fig. 8(a). The cathodic current decreases with increasing the DNS concentration, indicating the inhibition action of adsorbed DNS for the reduction process of silver ions. In addition, a common feature is that the current initially rises to the maximum and then decreases due to the nucleation and growth of the new phase. The wavelet analysis results show that although the energy in region A is increased with the increase of DNS concentration, the energy in region A is still relatively low compared with that in region C. Therefore, diffusion control is dominant at this time. According to the Scharifker–Hills model [40], when the $I-t^n$ curve of the rising part of current has a good linear relationship at $n=1/2$ or $3/2$, the explanation of the 3D nucleation model accompanied by the diffusion-controlled growth can be considered. As shown in the inset of Fig. 8(a), the $I-t^{3/2}$ curve of the rising part of current has a good linear relationship regardless of whether DNS is presented in the plating bath or not. Thus, the deposition of silver follows the 3D nucleation mode.

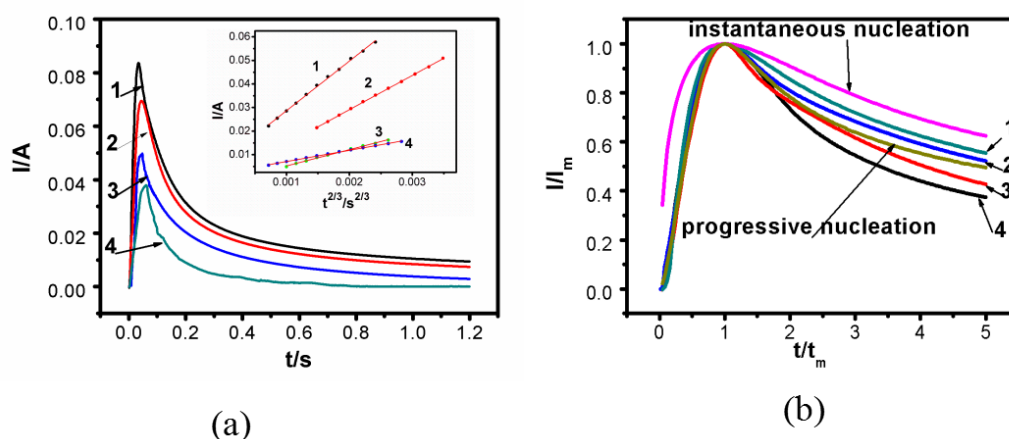


Figure 8. Potentiostatic current transients at -0.3v for silver deposition on copper from DNS bath in a series of DNS concentrations: 1-0mM; 2-0.5mM; 3-2mM; 4-6mM, inset: I vs. $t^{3/2}$ plots of the rising parts of the current transients: 1-0mM; 2-0.5mM; 3-2mM; 4-6mM. (b) Non-dimensional plots of I/I_m vs. t/t_m for -0.3v of silver deposition process from in a series of DNS concentrations bath: 1-0mM; 2-0.5mM; 3-2mM; 4-6mM.

By drawing the relationship curve between the normalized current I/I_m and time t/t_m , all current transients can be transformed into a dimensionless form. As shown in Fig. 8(b), instantaneous and progressive nucleation models have two theoretical curves [12, 26], respectively. They are often used for determining the nucleation mechanism on the basis of the experimental data.

For the instantaneous nucleation model:

$$\left(I/I_m\right)^2 = 1.9542/(t/t_m) \left[1 - \exp\left(-1.2564 \times (t/t_m)\right)\right]^2 \quad (1)$$

For the progressive nucleation model:

$$(I/I_m)^2 = 1.2254/(t/t_m) \left[1 - \exp(-2.3367 \times (t/t_m)^2) \right]^2 \tag{2}$$

where I_m and t_m represent the current and time coordinates of the peak value of Faraday current transient curve, respectively.

In Fig. 8(b), the nucleation of silver changes from partial instantaneous nucleation and partial progressive nucleation to complete progressive nucleation with the increase of DNS concentration.

If the nucleation model is progressive nucleation, the diffusion coefficient can be estimated from equation (3), where F is the Faraday constant, and C is the bulk concentration and D represents the diffusion coefficient of silver ion, respectively [12].

$$I_m^2 t_m = 0.2598(zFC)^2 D \tag{3}$$

The maximum number of nuclei (saturation nuclei number N_s) can also be obtained in accordance with Ref. [12]:

$$N_s = (AN_\infty / 2K'D)^{1/2} \tag{4}$$

$$AN_\infty = 4.6733 / t_m^2 \pi K'D \tag{5}$$

$$K' = 4/3(8\pi cM / \rho)^{1/2} \tag{6}$$

where AN_∞ represents the growth rate of nuclei, M is the molecular weight, and ρ is the density of silver deposit ($M=107.87$ g/mol and $\rho=10.5$ g/cm³).

The parameters' values at different DNS concentrations are calculated by the above formulas, as shown in Table 2. When the DNS concentration increases, the diffusion coefficient of silver ion exhibits an evident decrease. A complete adsorption film is gradually formed on the copper surface. This film increases the viscosity of interfacial solution and hinders transfer of silver ions between the solution and the interface. In addition, the nucleation rate AN_∞ and amount of nucleation point N_s show an evident decrease tendency with the increase of DNS concentration. The inhibition effect almost reaches the highest extent when the concentration of DNS increases to 2mM.

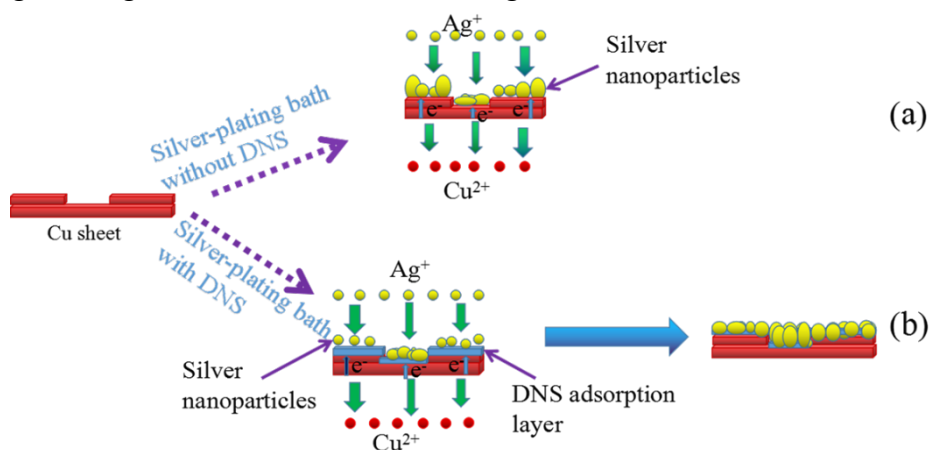
Table 2. Parameters calculated in accordance with equations (1)–(6) obtained from chronoamperometry at Cu in the methanesulfonic acid baths under a series of DNS concentrations.

C (mM)	t_m (s)	I_m (A)	$I_m^2 t_m$ (A ² s)	D (cm ² s ⁻¹)	AN_∞ (cm ² s ⁻¹)	N_s (cm ² s ⁻¹)
0	0.034	0.0846	2.494×10^{-4}	1.049×10^{-7}	8.635×10^7	5.234×10^6
0.5	0.049	0.0697	2.035×10^{-4}	0.827×10^{-7}	6.439×10^7	2.493×10^6
2	0.055	0.0527	1.631×10^{-4}	0.736×10^{-7}	5.482×10^7	3.261×10^6
6	0.067	0.0384	1.017×10^{-4}	0.418×10^{-7}	6.293×10^7	2.843×10^6

3.6 Silver deposition hypothesis

There are some researchers discussed the mechanism for silver deposition. Adachi et al. [34] discussed the mechanism of smooth Ag plating by virtue of its electrochemical and diffusive properties. They considered that the leveling of the silver plating surface was associated with electrochemical

properties such as the exchange current density and equilibrium potential of the redox reaction. In addition, diffusive properties such as thickness of the diffusion layer are also related to the roughness of the surface. Liu et al. [41] thought that the charge transfer process controls the reaction kinetics at the early stages of Ag electrodeposition, indicating that the nucleation stage of Ag crystallization precedes the growth of the Ag deposit. In addition, the nucleation process of silver deposition is a typical 3-D multiple nucleation process controlled by hemispheric diffusion toward the nucleation centers on the cathode. However, we proposed the hypothesis of displacement silver plating on copper sheets. Copper is immediately oxidized when it contacts with a silver-containing plating solution owing to the large potential difference between copper and silver. Lost electrons are transferred from the copper matrix to the interface, whereas silver ions diffuse from the bulk solution to the copper sheet and obtain electrons at the interface of the copper/plating solution, leading to the deposition of silver on the copper surface. However, even polished copper surfaces have micro-inhomogeneity. When the silver ions transfer to the copper/plating solution interface, the concentration of silver ions at the pit sites on the copper surface is lower than that of the protrusion sites because the thickness of the diffuse layer in pit sites is larger than that in protrusion sites. Hence, the deposition speed of silver in pit sites is lower than that in protrusion sites, increasing the height difference and surface roughness, as described in Scheme 1(a).



Scheme 1. Mechanism of DNS effect on displacement silver plating on copper

When DNS is added to the plating bath, the concentration of DNS at the pit sites on the copper surface will be lower than that of the protrusion sites because the thickness of the DNS diffuse layer in the pit site is larger than that in the protrusion sites. When the concentration of DNS at the protrusion site reaches the critical value, a complete adsorption film will be formed on the protrusion site of the copper surface. This film will evidently inhibit the electron transfer from the copper matrix to its interface (i.e., the anodic process). By contrast, the relatively low concentration of DNS at the pit site complicates the formation of a complete adsorption film, resulting in a weak inhibition of electron transfer from the copper matrix to the interface. Meanwhile, the adsorption film hinders silver ions from obtaining electrons (i.e., cathodic process) from the copper/plating solution interface. The complete adsorption membrane has greater hindrance to electron transfer than the incomplete adsorption membrane. Therefore, the deposition speed of silver at the protrusion site on surfaces of the copper will

be lower than that of the pit site. As such, the height difference of uneven surface is gradually reduced, and a smooth and fine silver-plating layer is finally obtained, as shown in Scheme 1(b).

4. CONCLUSIONS

The addition of DNS in a displacement copper plating bath is helpful to obtain a bright and smooth silver coating. In this work, the effect of 3,5-dinitrosalicylic acid (DNS) on displacement silver plating on copper substrate in methanesulfonic acid is studied. The main conclusions are as follows:

(1) The electrochemical research results show that DNS inhibits the anodic dissolution of copper and also prevents silver ions from obtaining electrons from the interface between the copper matrix and plating solution by forming an adsorption layer.

(2) In a silver deposition with the 3D nucleation mode, the maximum current value of Faraday decreases with increasing the DNS concentration and the nucleation rate of silver and the diffusion coefficient of silver ions decrease.

(3) In addition, the DNS concentration in the protruding sites is higher than that in the pit sites because of the large diffusion layer thickness. As a result, the deposition rate of silver ions at the pit sites is faster than that in the protrusion sites.

(4) New crystal nuclei continuously grow at the pit sites and the nucleation mechanism of silver changes toward to the progressive nucleation. The change of cell energy calculated by wavelet transform shows that the addition of DNS can change the control process of the silver deposition process to activation control from original diffusion control.

ACKNOWLEDGEMENTS

This work was financially supported by the Changsha Municipal Science and Technology Program (NO. kq1907095) and the Strategic Emerging Industry Scientific and Technological Research and Major Achievements Transformation Project of Hunan Province (NO. 2019GK4041).

References

1. X.G. Cao and H.Y. Zhang, *Powder Technol.*, 226 (2012) 53.
2. D.S. Jung, H.M. Lee and Y.C. Kang, *J. Colloid. Interf. Sci.*, 364 (2011) 574.
3. Y.L. Zhou, Y.Li, Y.Y. Chen and M. Zhu, *IEEE Trans. Device. Mater. Reliab.*, 19 (2019) 622.
4. X. Yu, J. Li and T.A. Shi, *J. Alloy. Compd.*, 724 (2017) 365.
5. K. Xiao, P. Yi, L. D. Yan, Z. H. Bai, C. F. Dong, P. F. Dong, X. Gao. *Materials*, 10 (2017) 762.
6. H.T. Hai, J.G. Ahn and D.J. Kim. *Surf. Coat. Tech.*, 201 (2006) 3788.
7. J. Zhao, D. Zhang and X. Song, *App. Surf. Sci.*, 258 (2012) 7430.
8. P.Y. Sark, C. Y. An and P.K. Kannan, *App. Surf. Sci.*, 389 (2016) 865.
9. S.G. Warriar and R.Y. Lin, *J. Mater. Sci.*, 28 (1993) 4868.
10. V.V. Levenets, R.E. Amaya and N.G. Tarr, *Solid. State Electron.*, 50 (2006) 1389.
11. G.M.D. Oliveira, L.L. Barbosa and R.L. Broggi, *J. Electroanal. Chem.*, 578 (2005) 151.
12. Z.B. Lin, B.G. Xie and J.S. Chen, *J. Electroanal. Chem.*, 633 (2009) 207.

13. G. M. Zarkadas, A. Stergiou and G. Papanastasiou, *Electrochim. Acta*, 50 (2005) 5022.
14. O. Aaboubi and A. Housni, *J. Electroanal. Chem.*, 677-680 (2012) 63.
15. Y. J. Hu, H. Y. Zhang and X.L. Cheng, *App. Surf. Sci.*, 257 (2011) 2813.
16. D. Yu, G. Kang and W. Tian, *App. Surf. Sci.*, 357 (2015) 1157.
17. S. Mu, H. Xie and W. Wang, *App. Surf. Sci.*, 353 (2015) 608.
18. B. Huang, W. Gan and G. Guo, *Ceram. Int.*, 40 (2014) 393.
19. D.-X. Wu, Y.-W. Wang, Z.-L. Xiao, R.-H. Yang and W.-J. Yao, *Surf. Tech.*, 48 (2019) 301.
20. D.-X. Wu, R.-H. Yang, Z.-L. Xiao, Y.-W. Wang, W.-J. Yao, G.-H. Zhou and W.-Y. Wang, *Surf. Tech.*, 48 (2019) 266.
21. D.-X. Wu and Y. Liu, *Rare Metal. Mat. Eng.*, 41 (2012) 681.
22. J.I. Njagi, C.M. Netzband and D.V. Goia, *J. Colloid. Interf. Sci.*, 488 (2017) 72.
23. X. Xu, X. Luo, H. Zhuang, W. Li and B. Zhang, *Mater. Lett.*, 57 (2003) 3987.
24. D. Gonnissen, A. Hubin and J. Vereecken, *Electrochim. Acta*, 44 (1999) 4129.
25. S. Vandeputte, A. Hubin and J. Vereecken, *Electrochim. Acta*, 42 (1997) 3429.
26. S. Vandeputte, E. Verboom and A. Hubin, *J. Electroanal. Chem.*, 397 (1995) 249.
27. J.F. Lu, M.Z. An and H. Zhang, *Rare Metals*, 25 (2006) 255.
28. M. Miranda-Hernández and I. González, *Electrochim. Acta*, 42 (1997) 2295.
29. W.-J. Yao, D.-X. Wu, Z.-L. Xiao, Y.-W. Wang and R.-H. Yang, *Int. J. Electrochem. Sci.*, 14 (2019) 9633.
30. Y. Wang, D. Li, J.-F. Kang, S.-Y. Guan and D.-X. Wu, *Int. J. Electrochem. Sci.*, 14 (2019) 5448.
31. D. Li, F. Xie and J. Zhang, *Electroanal.*, 30 (2018) 2413.
32. C.Z. Lv, D. Chen, Z. Cao, F. Liu, X.M. Cao, J.L. He and W.Y. Zhao, *Int. J. Electrochem. Sci.*, 11 (2016) 10107.
33. Z. Zhang, W. H. Leng and Q.Y. Cai, *J. Electroanal. Chem.*, 578 (2005) 357.
34. K. Adachi, A. Kitada, K. Fukami and K. Murase, *J. Electrochem. Soc.*, 66 (2019) D409.
35. M. Korabik, L. Martika and M. Koman, *Inorg. Chem. Commun.*, 7 (2004) 548.
36. J.A. Switzer, C.J. Hung and L.Y. Huang, *J. Am. Chem. Soc.*, 120 (1998) 3530.
37. E.W. Bohannan, L.Y. Huang and S. Miller, *Langmuir*, 15 (1999): 813.
38. E. Budevski, W. Obretenov and W. Bostanov, *Electrochim. Acta*, 34 (1989) 1023.
39. W. Xiao, Y. Lei, Z. Xia, X. Chen, Y. Han and J. Nie, *J. Alloy. Compd.*, 724 (2017) 24.
40. B. Scharifker, *Electrochim. Acta*, 28 (1983) 879.
41. A. Liu, X. Ren and M. An, *New J. Chem.*, 41 (2017) 11104.